Morphological Degradation in Low Bandgap Polymer SolarCells – An In Operando Study

*Christoph J. Schaffer, Claudia M. Palumbiny, Martin A. Niedermeier, Christian Burger, Gonzalo Santoro, Stephan V. Roth, and Peter Müller-Buschbaum**

During the last decades, different types of promising photovoltaic devices have opened new fields of application beyond conventional silicon based solar cells (SCs). Especially, the mechanical flexibility of thin-film SCs renders them highly promising as application on curved surfaces, such as in modern architecture. Thin film SCs cover a wide range of solar cell types in which electricity is generated in purely inorganic (e.g., a-Si, copper indium gallium diselenide (CIGS), CdTe), hybrid organic/inorganic (e.g., dye sensitized, organometal halide perovskite), or purely organic structures (e.g., polymer–fullerene bulk-heterojunctions (BHJ). For a decent overview of state-of-the-art solar cell technologies and their typical performance, we refer to the literature.[1]

Although organic SCs feature lower power conversion efficiencies (PCE) than some of their inorganic competitors in the thin-film field, they offer several unique features. The biggest advantage is hereby the ease of production. Particularly BHJ SCs based on semiconducting polymers and fullerenes can be manufactured purely by cost-effective wet-chemical methods such as roll-to-roll printing.[2–7] Thereby, only abundant and nontoxic materials are necessary. Furthermore, a wide range of suitable materials allows for production of semitransparent photovoltaics with different colors. This broadens the scope for application in architecture on a large scale. The use of processing additives has been shown to drastically improve the power conversion efficiencies of several polymer–fullerene solar cells whose record efficiencies have recently been pushed beyond the milestone of 10%.[8–10]

C. J. Schaffer, Dr. C. M. Palumbiny,
Dr. M. A. Niedermeier, C. Burger,
Prof. P. Müller-Buschbaum
Technische Universität München
Physik-Department
Lehrstuhl für Funktionelle Materialien
James-Franck-Str. 1, D-85748 Garching, Germany
E-mail: muellerb@ph.tum.de
Dr. G. Santoro
Instituto de Ciencia de Materiales de Madrid
ICMM-CSIC
Sor Juana Inés de la Cruz 3, 28049 Madrid, Spain
Prof. S. V. Roth
Deutsches Elektronen-Synchrotron DESY
Notkestr. 85, D-22607 Hamburg, Germany
Prof. S. V. Roth
Department of Fibre and Polymer Technology
KTH Royal Institute of Technology
Teknikringen 56-58, Stockholm SE-100 44, Sweden

In the active layer of polymer–fullerene BHJ SCs, interpenetrating polymer and fullerene domains form by phase segregation during active layer deposition. The resulting structure is referred to as the BHJ. In most material combinations, polymer domains conduct positive charge carriers and fullerene domains conduct negative charge carriers. Under operation, photons are absorbed by the polymer and thereby excitons, i.e., bound electron–hole pairs, are created. In order to produce electricity, the exciton must be split into free charge carriers which subsequently must move through the respective material domain network to the contacts. However, exciton splitting is only possible if the exciton reaches a polymer–fullerene interface. An exciton can only diffuse on a characteristic length-scale on the order of 10 nm in the polymer. Thus, the nanostructure of interpenetrating domains plays a crucial role for solar cell functioning and therefore must be optimized:[11–17] If the structure is too coarse, excitons will not reach an interface and will not be split. If the structure is too fine, excitons will be easily split but the charge carriers will be trapped in island domains or due to domain impurities in case of excessive molecular mixing.

In the special case of PCPDTBT[18]:$PC_{71}BM$ (poly[2,1,3-benzothiadiazole-4,7-diyl[4,4-bis[2-ethylhexyl]- 4H-cyclopenta[2,1-b:3,4-b′] dithiophene-2,6-diyl]], [6,6]-phenyl C_{71} butyric acid methyl ester), we have recently shown that the use of 1,8-octanedithiol (ODT) as processing additive enhances microphase separation and therefore leads to coarsening in the nanostructure of the active polymer–fullerene bulk-hetero- junction.[14] This behavior was also suggested for similar mate-rial combinations with different solvent additives.[19–22] By this mechanism, the PCE is boosted from 2.5% to 5.8%.[23] It is, though, not clear if such an optimized morphology is stable, particularly since it was shown that solvent additives can affect the degradation behavior.[24,25]

Although it had been widely assumed that the morphology of a BHJ is generally not stable with time, the first experimental evidence was given in our previous work on polythiophene based SCs.[13] We pioneered probing simultaneously the evolution of both, the nanometer-scaled morphology of the BHJ in the active layer of the solar cell and the photovoltaic character- istics of a running polymer–fullerene solar cell as a function of time.[13] This was achieved by combining in situ (microfocused) grazing-incidence small angle X-ray scattering (μGISAXS) with current–voltage tracking (*IV*) on a P3HT:PCBM solar cell. We could quantitatively link the observed coarsening of morphology with the decay in the current-output and thus evi- denced morphological degradation in BHJ SCs. It is noteworthythat the P3HT:PCBM blend naturally tends to demix whereas inhighly efficient blend systems used for organic solar cells, such

as PCPDTBT:$PC_{71}BM$ or PTB7:$PC_{71}BM$, a processing additive is needed to adjust phase separation. Hence, the question arises if and how the use of processing additives affects the morphological degradation behavior of such modern devices.

In this work, we address the morphological instability of a model low bandgap polymer–fullerene BHJ solar cell fabricated with a high boiling point processing additive which enhances microphase separation: For the first time, we present an in operando μGISAXS study on a PCPDTBT:$PC_{71}BM$ solar cell processed from chlorobenzene blended with 3 vol% ODT as high boiling point processing additive. This experiment reveals simultaneous information on both, the morphology of the active layer and its photovoltaic characteristics in real-time. The conclusions drawn from the real-time investigation are complemented with UV–visible-light absorption spectroscopy (UV–vis) on plain active layers processed with and without ODT.

To probe both, the nanometer-scale morphology of an organic solar cell active layer and its photovoltaic character- istics, a home-built measurement chamber is implemented in a beamline at a synchrotron radiation facility (beamline P03, DESY Hamburg, Germany).[26] The high X-ray brilliance therein provides a reasonable time resolution which allows for real-time monitoring of dynamic processes in the morphology of thin films.[4,13,27–29] The structural information of the active layer is probed using μGISAXS. This technique allows to probe structures with length scales varying from a few up to a few hundreds of nanometers on a macroscopic sample area.[29–33] In order to suppress scattering from the electrodes and local heterogeneities, μGISAXS patterns are recorded next to (but not on top of) the electrodes. For the measurement, the solar cell is mounted in the measurement chamber and vacuum is applied to suppress degradation by oxidation. Through a window, simulated sunlight can enter the chamber and illuminate the solar cell. An electric feedthrough enables *IV*-tracking of the solar cell during the experiment. Furthermore, Peltier elements are used to constantly cool the active layer below 50 °C. X-rays enter and exit the measurement chamber through polyimide win- dows. Additional information on the setup is given in sectionS1 of the Supporting Information.

Before the solar cell is exposed to simulated sunlight, a reference μGISAXS measurement is performed. *IV*-trackingis started and a current–voltage curve is recorded perpetually every 16 s. Illumination begins subsequently. μGISAXS measurements are taken after 2, 6, 11, 31, 62, 139, 178, 239, 300, 360, and 421 minutes of illumination. In order to suppress X-ray induced damage of the active layer, each measurement islimited to an exposure time of 2 s.

In μGISAXS experiments, a microfocused X-ray beam impinges the sample under a shallow angle that exceeds the critical angle of total reflection for all probed materials. Depending on the inner film structure of the probed mate-rial, the beam is diffusely scattered and detected by a 2D area detector.

Figure 1 shows scattering images at the different times before and after illumination started. Strong scattering is observed when the refractive indices of the materials in the probed film differ strongly from each other. This is the case when the film consists of separated domains instead of a homo-geneous blend. In Figure 1, the scattering intensity starts to

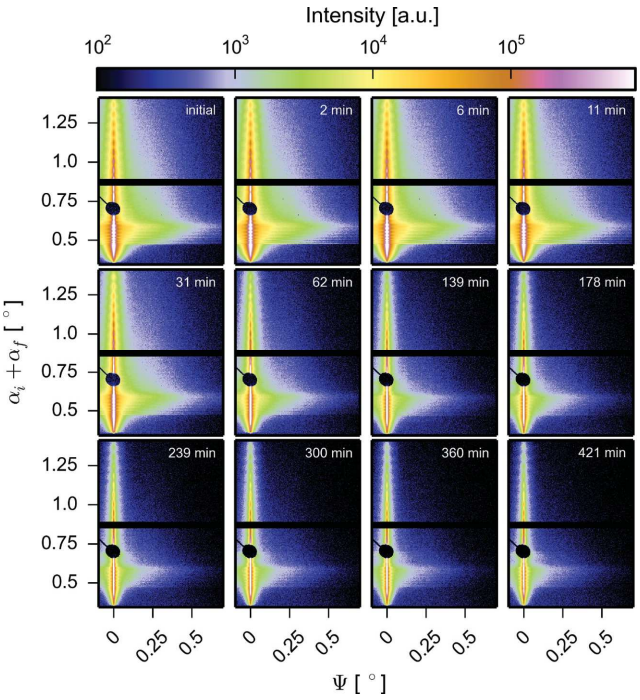

Figure 1. μGISAXS patterns after different illumination times. α_i+α_f describes the exit angle with respect to the incoming X-ray beam. Ψ describes the horizontal angle. The black shadow at $\alpha_i + \alpha_f \approx 0.7°$ arises from the specular beam blocker which is used to prevent damage due to high flux to the detector. The black line above is an inter-array detector gap.

drop visibly after 12 min. We propose that this drop is caused by a loss of scattering contrast which occurs when the active layer structure blurs (other potential reasons are ruled out in Section S2 of the Supporting Information.) This observa-tion is in contradiction with the findings by Waters et al., who suggest enhanced $PC_{71}BM$ agglomeration after 300 h of light soaking.[25] However, it is noteworthy that identical morphologies were thereby found for fresh films in both cases, with and without ODT, which disagrees with common literature where enhanced phase separation is found due to various solvent additives, including ODT.[14,19–21] A particularly high scattering intensity appears when the beam scatters under the criticalangle of a certain film component with respect to the sample surface. This is referred to as the so-called Yoneda peak.[34] By analyzing the diffusely scattered intensity at the critical angle ofPCPDTBT at 0.12°, information on the polymer domain struc- ture is detected. To obtain this information, horizontal line cuts are integrated over an exit angle range of 0.12°–0.13°. The dataare modeled in the framework of the effective interface approximation and local monodisperse approximation.[35,36] In order to approximate the data sufficiently, three hierarchical substructures need to be assumed (see section S3, Supporting Information). One substructure with very large domains (>100 nm) exceeds the length scale of exciton diffusion and therefore does not play a significant role in photovoltaic devices. Thus, such large structures are not further discussed. The focus is put on two further substructures revealed by modeling with domain radii on the order of a few (R_{small}) up to a few tens (R_{med}) of

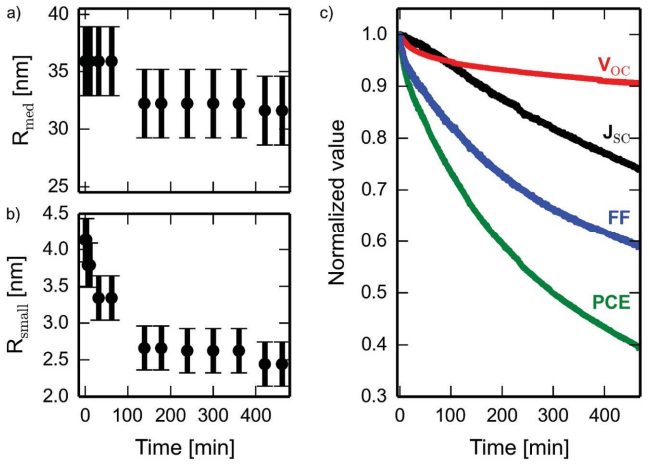

Figure 2. Time evolution of morphological and photovoltaic parameters. a) Temporal evolution of medium-sized and b) small-sized polymer domains as obtained from μGISAXS data modeling. c) Normalized photovoltaic characteristics extracted from *IV*-tracking: Open-circuit voltage (V_{OC}), short-circuit current density (J_{SC}), fill factor (FF), and power conversion efficiency (PCE). Error bars are estimated from fitting tolerances.

nanometers. The evolution of these domain sizes is depicted in **Figure 2**a,b.

Both domain sizes shrink with operation time. Especially, the small domains R_{small} show a strong decay in size with time. We propose that these shrinking domains lose their connection to the interpenetrating network. Thus, with diminishing domain size the number of recombination sites for nongeminate recombination increases: Although the splitting chanceof excitons grows, the extraction probability for free charge carriers drops because charge carriers get trapped in isolated domains. The resulting amplification of recombination will lower the fill factor of the solar cell. Exactly this behavior is observed in our experiment. Figure 2c shows the evolution of the photovoltaic parameters of the solar cell as a function of operation time. Although open-circuit voltage (V_{OC}) and short- circuit current density (J_{SC}) drop with time, we find that thefill factor (FF) degrades the strongest and therefore plays the key role in solar cell degradation. All in all, we propose that the domain structure of the active layer refines during opera- tion and leads to a decrease of device performance. We find particularly noteworthy that the domain sizes on a length scale of a few nanometers diminish by a factor of roughly two. We have recently shown that PCPDTBT:$PC_{71}BM$ blend thin films processed with ODT show double domain sizes on this very length scale, as compared to films processed without ODT.[14] This fact suggests that residual ODT evaporates from the film during our experiment and that without the further presence of ODT, the active layer morphology changes toward the one without ODT. A loss of ODT during our experiment is further supported by the scattering data (cf. section S4, Supporting Information). It is important to note that the system is never in thermodynamic equilibrium but changes from one nonequilibrium state to another. In order to support this hypothesis, we complement the data with UV–vis absorption spectroscopy on PCPDTBT:$PC_{71}BM$ films processed with and without ODT after different storage times. These are shown in section S5

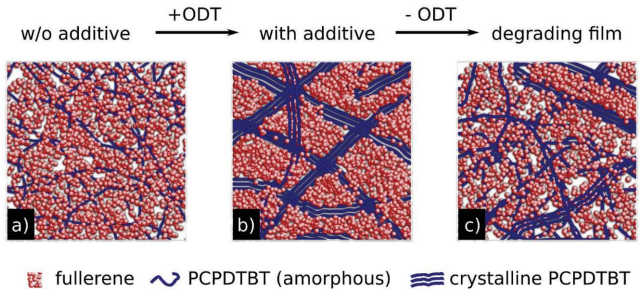

Figure 3. Illustration of the model for morphological degradation in PCPDTBT:$PC_{71}BM$ thin films. a) Films without ODT show fine mixing. b) When films are processed with ODT, phase separation occurs (reversibly) and sharp domains form. c) When ODT leaves the film, the morphology reverts toward the state without ODT. This implies mixing of PCPDTBT and $PC_{71}BM$.

and Figure S6 of the Supporting Information. While the film without ODT shows no significant changes with time, the film processed with ODT turns out to converge to the spectra without ODT. Since the absorption feature at 800 nm emerges from well-ordered polymer domains,[14] we infer that the mor- phology of the blend thin film with ODT reverts toward the morphology of films processed without ODT. This process is strongly accelerated for our in situ experiment due to the applied vacuum and the elevated film temperature.

Figure 3 schematically describes our model in which the processing additive enhances reversible microphase separation and leads to a blurred domain structure when evaporating from the film, meaning that one nonequilibrium state changes into another one.

In summary, we suggest that the processing-additive-induced microphase separation between polymer (PCPDTBT) and fullerene ($PC_{71}BM$), which generates percolation in the active layer, is reversible. During operation, the residual sol- vent additive evaporates from the active layer of the solar cell. Thus, the BHJ blurs and islands form. Consequently, charge carrier recombination fortifies and causes deterioration of the fill factor. This mechanism leads to solar cell degradation. It is speculated that morphological instabilities caused by evapora- tion of processing agents applies for all organic solar cells fab- ricated with volatile solvent additives. Therefore, special focus should be put on morphologically stabilizing such solar cells by actively retaining the solvent additive inside the active layer.We suggest that such stabilization could potentially be achievedby suitable encapsulation techniques or chemically binding sol-vent additives to one of the active materials.

Experimental Section

Solar cells were prepared by spin coating a PCPDTBT:PC71BM (1:2.7 by weight, 25 mg mL^{-1} total concentration, both supplied by ONE-material Inc. and used as delivered, M_W = 31 kDa, polydispersity index (PDI) = 1.9) solution from chlorobenzene:1,8-octanedithiol (3 vol%) on a poly(ethylenedioxythiophene):poly(styrenesulfonate) (denoted PEDOT:PSS, filtered with 0.45 μm poly(vinylidenefluoride) filter, annealed for 10 min @ 140 °C) covered indium-doped tin oxide (ITO) substrate (Solems). Al electrodes were applied by physical vapor deposition (PVD) at a pressure of 2×10^{-5} mbar. Samples were sealed in KF flange steel

containers inside an Ar-filled glove box (<0.1 ppm O_2 and H_2O) in order to minimize degradation during transport to the synchrotron facility (5 d storage time). The solar cell encountered air exposure for <10 min while mounting in the measurement chamber. The in operando µGISAXS experiment was performed at beamline P03 of the PETRA III storage ring at DESY, Hamburg, Germany.[26] An incident angle of 0.35° was chosen with a photon energy of 11 keV, a sample-detector distance of 3698 mm, and a beam size of 28×23 µm^2. A Pilatus 300k area detector with a pixelsize of 0.172 mm was used. For illumination, a Perkin Elmer PX5 150 WXenon lamp was coupled into the evacuated (<0.5 mbar) measurementchamber via a mirror with a constant (+/–3%) intensity of ≈100 W cm^{-2}. All scattering data were normalized to the momentary beam intensity. *IV* curves were measured using a Keithley Series 2400 Sourcemeter. UV–vis samples were prepared on glass substrates (cleaned in an acid bath according to literature)[37] by spin coating blend solution as described above. Spectrograms were recorded using a PerkinElmer Lambda35 at a scanning speed of 120 nm min^{-1}, a slit width of 2 nm, and a resolution of 1 nm. UV–vis data had been corrected for the absorbance of a cleaned glass substrate. The samples were stored under dark ambient conditions.

Acknowledgements

This work was financially supported by TUM Solar in the frame of the Bavarian Collaborative Research Project “Solar technologies go Hybrid” (SolTec), the GreenTech Initiative (Interface Science for Photovoltaics – ISPV) of the EuroTech Universities, and the Nanosystems Initiative Munich (NIM). C.J.S. thanks the Bavarian State Ministry of Sciences, Research and Arts for funding this work via the International Graduate School “Materials Science of Complex Interfaces” (CompInt) and Dr. Matthias A. Ruderer for discussion and preliminary work. C.M.P. acknowledges financial support by the “International Graduate School of Science and Engineering” (IGSSE).

[1] M. A. Green, K. Emery, Y. Hishikawa, W. Warta, E. D. Dunlop, *Prog. Photovoltaics* **2015**, *23*, 1.
[2] R. Søndergaard, M. Hösel, D. Angmo, T. T. Larsen-Olsen, F. C. Krebs, *Mater. Today* **2012**, *15*, 36.
[3] F. C. Krebs, *Sol. Energy Mater. Sol. Cells* **2009**, *93*, 394.
[4] S. Pröller, F. Liu, C. Zhu, C. Wang, T. P. Russell, A. Hexemer, P. Müller-Buschbaum, E. M. Herzig, *Adv. Energy Mater.* **2016**, *6*, 1501580.
[5] G. Dennler, M. C. Scharber, C. J. Brabec, *Adv. Mater.* **2009**, *21*, 1323.
[6] C. Deibel, V. Dyakonov, *Rep. Prog. Phys.* **2010**, *73*, 096401.
[7] H. Hoppe, N. S. Sariciftci, *J. Mater. Res.* **2004**, *19*, 1924.
[8] Z. A. Page, Y. Liu, V. V. Duzhko, T. P. Russell, T. Emrick, *Science* **2014**, *346*, 441.
[9] Y. Liu, Z. A. Page, T. P. Russell, T. Emrick, *Angew. Chem., Int. Ed.* **2015**, *54*, 11485.
[10] S.-H. Liao, H.-J. Jhuo, P.-N. Yeh, Y.-S. Cheng, Y.-L. Li, Y.-H. Lee, S. Sharma, S.-A. Chen, *Sci. Rep.* **2014**, *4*, 6813.
[11] D. Huang, Y. Li, Z. Xu, S. Zhao, L. Zhao, J. Zhao, *Phys. Chem. Chem. Phys.* **2015**, *17*, 8053.
[12] D. Chirvase, J. Parisi, J. C. Hummelen, V. Dyakonov, *Nanotechnology* **2004**, *15*, 1317.
[13] C. J. Schaffer, C. M. Palumbiny, M. A. Niedermeier, C. Jendrzejewski, G. Santoro, S. V. Roth, P. Müller-Buschbaum, *Adv. Mater.* **2013**, *25*, 6760.
[14] C. J. Schaffer, J. Schlipf, E. Dwi Indari, B. Su, S. Bernstorff, P. Müller-Buschbaum, *ACS Appl. Mater. Interfaces* **2015**, *7*, 21347.
[15] H. Yan, B. A. Collins, E. Gann, C. Wang, H. Ade, C. R. McNeill, *ACS Nano* **2012**, *6*, 677.
[16] Y. Kim, S. A. Choulis, J. Nelson, D. D. C. Bradley, S. Cook, J. R. Durrant, *Appl. Phys. Lett.* **2005**, *86*, 063502.
[17] G. Li, Y. Yao, H. Yang, V. Shrotriya, G. Yang, Y. Yang, *Adv. Funct. Mater.* **2007**, *17*, 1636.
[18] S. H. Park, A. Roy, S. Beaupre, S. Cho, N. Coates, J. S. Moon, D. Moses, M. Leclerc, K. Lee, A. J. Heeger, *Nat. Photonics* **2009**, *3*, 297.
[19] Y. Gu, C. Wang, T. P. Russell, *Adv. Energy Mater.* **2012**, *2*, 683.
[20] H.-C. Liao, C.-S. Tsao, Y.-T. Shao, S.-Y. Chang, Y.-C. Huang, C.-M. Chuang, T.-H. Lin, C.-Y. Chen, C.-J. Su, U.-S. Jeng, Y.-F. Chen,W.-F. Su, *Energy Environ. Sci.* **2013**, *6*, 1938.
[21] F. Etzold, I. A. Howard, N. Forler, D. M. Cho, M. Meister, H. Mangold, J. Shu, M. R. Hansen, K. Müllen, F. Laquai, *J. Am. Chem. Soc.* **2012**, *134*, 10569.
[22] Z. Li, C. R. McNeill, *J. Appl. Phys.* **2011**, *109*, 074513.
[23] J. Peet, J. Y. Kim, N. E. Coates, W. L. Ma, D. Moses, A. J. Heeger, G. C. Bazan, *Nat. Mater.* **2007**, *6*, 497.
[24] W. Kim, J. K. Kim, E. Kim, T. K. Ahn, D. H. Wang, J. H. Park, *J. Phys. Chem. C* **2015**, *119*, 5954.
[25] H. Waters, N. Bristow, O. Moudam, S.-W. Chang, C.-J. Su, W.-R. Wu, U.-S. Jeng, M. Horie, J. Kettle, *Org. Electron.* **2014**, *15*, 2433.
[26] A. Buffet, A. Rothkirch, R. Döhrmann, V. Körstgens, M. M. Abul Kashem, J. Perlich, G. Herzog, M. Schwartzkopf, R. Gehrke, P. Müller-Buschbaum, S. V. Roth, *J. Synchrotron Radiat.* **2012**, *19*, 647.
[27] K. W. Chou, B. Yan, R. Li, E. Q. Li, K. Zhao, D. H. Anjum, S. Alvarez, R. Gassaway, A. Biocca, S. T. Thoroddsen, A. Hexemer, A. Amassian, *Adv. Mater.* **2013**, *25*, 1923.
[28] J. T. Rogers, K. Schmidt, M. F. Toney, G. C. Bazan, E. J. Kramer, *J. Am. Chem. Soc.* **2012**, *134*, 2884.
[29] S. V. Roth, G. Herzog, V. Körstgens, A. Buffet, M. Schwartzkopf, J. Perlich, M. M. A. Kashem, R. Döhrmann, R. Gehrke, A. Rothkirch, K. Stassig, W. Wurth, G. Benecke, C. Li, P. Fratzl, M. Rawolle, P. Müller-Buschbaum, *J. Phys.: Condens. Matter* **2011**, *23*, 254208.
[30] P. Müller-Buschbaum, *Adv. Mater.* **2014**, *26*, 7692.
[31] D. Smilgies, P. Busch, C. M. Papadakis, D. Posselt, *Synchrotron Radiat. News* **2002**, *15*, 35.
[32] S. V. Roth, M. Burghammer, C. Riekel, P. Müller-Buschbaum, A. Diethert, P. Panagiotou, H. Walter, *Appl. Phys. Lett.* **2003**, *82*, 1935.
[33] E. Verploegen, C. E. Miller, M. F. Toney, *Synchrotron Radiat. News* **2010**, *23*, 16.
[34] Y. Yoneda, *Phys. Rev.* **1963**, *131*, 2010.
[35] R. Lazzari, *J. Appl. Crystallogr.* **2002**, *35*, 406.
[36] G. Renaud, R. Lazzari, F. Leroy, *Surf. Sci. Rep.* **2009**, *64*, 255.
[37] P. Müller-Buschbaum, *Eur. Phys. J. E* **2004**, *12*, 443.